AMERICAN SOCIETY FOR MICROBIOLOGY | Journal of Virology®

CELLULAR RESPONSE TO INFECTION

Syk Facilitates Influenza A Virus Replication by Restraining Innate Immunity at the Late Stage of Viral Infection

Yingying Li,[a,b] Shasha Liu,[a,c] Yuhai Chen,[a] Biao Chen,[a,b] Meng Xiao,[a,c] Bincai Yang,[c] Kul Raj Rai,[a,c] Mohamed Maarouf,[a] Guijie Guo,[a,c] Ji-Long Chen[c]

[a]CAS Key Laboratory of Pathogenic Microbiology and Immunology, Institute of Microbiology, Chinese Academy of Sciences (CAS), Beijing, China
[b]University of Chinese Academy of Sciences, Beijing, China
[c]Key Laboratory of Fujian-Taiwan Animal Pathogen Biology, College of Animal Sciences, Fujian Agriculture and Forestry University, Fuzhou, China

ABSTRACT Spleen tyrosine kinase (Syk) has recently come forth as a critical regulator of innate immune response. Previous studies identify Syk as a key kinase for STAT1 activation at the early stage of influenza A virus (IAV) infection that is involved in initial antiviral immunity. However, the involvement of Syk in host antiviral immunity during the late phase of IAV infection and its effect on pathogenesis of the virus remain unknown. Here, we found through time course studies that Syk restrained antiviral immune response at the late stage of IAV infection, thereby promoting viral replication. Depletion of Syk suppressed IAV replication *in vitro*, whereas ectopic expression of Syk facilitated viral replication. Moreover, Syk-deficient mice were employed, and we observed that knockout of Syk rendered mice more resistant to IAV infection, as evidenced by a lower degree of lung injury, slower body weight loss, and an increased survival rate of Syk knockout mice challenged with IAV. Furthermore, we revealed that Syk repressed the interferon response at the late stage of viral infection. Loss of Syk potentiated the expression of type I and III interferons in both Syk-depleted cells and mice. Mechanistically, Syk interacted with TBK1 and modulated its phosphorylation status, thereby impeding TBK1 activation and restraining innate immune signaling that governs interferon response. Together, these findings unveil a role of Syk in temporally regulating host antiviral immunity and advance our understanding of complicated mechanisms underlying regulation of innate immunity against viral invasion.

IMPORTANCE Innate immunity must be tightly controlled to eliminate invading pathogens while avoiding autoimmune or inflammatory diseases. Syk is essential for STAT1 activation at the early stage of IAV infection, which is critical for initial antiviral responses. Surprisingly, here a time course study showed that Syk suppressed innate immunity during late phases of IAV infection and thereby promoted IAV replication. Syk deficiency enhanced the expression of type I and III interferons, inhibited IAV replication, and rendered mice more resistant to IAV infection. Syk impaired innate immune signaling through impeding TBK1 activation. These data reveal that Syk participates in the initiation of antiviral defense against IAV infection and simultaneously contributes to the restriction of innate immunity at the late stage of viral infection, suggesting that Syk serves a dual function in regulating antiviral responses. This finding provides new insights into complicated mechanisms underlying interaction between virus and host immune system.

KEYWORDS influenza A virus, innate immunity, spleen tyrosine kinase, interferon, TBK1

Influenza A virus (IAV) infection causes seasonal epidemics and occasional pandemics, posing a great threat to global public health (1–3). The host innate immune system provides the first line of defense against invading pathogens. Upon IAV infection, the conserved viral components, called pathogen-associated molecular patterns (PAMPs), are sensed by cellular pattern recognition receptors (PRRs), such as Toll-like receptors (TLRs), retinoic acid inducible gene-I (RIG-I)-like receptors (RLRs), and nucleotide-binding oligomerization domain (NOD)-like

Editor Anice C. Lowen, Emory University School of Medicine

Address correspondence to Guijie Guo, chenjl@im.ac.cn, or Ji-Long Chen, chenjl@im.ac.cn.

The authors declare no conflict of interest.

Received 27 January 2022
Accepted 18 February 2022
Published 16 March 2022

receptors (NLRs) (4–6). The activated PRRs trigger downstream signaling cascades, including the recruitment and activation of TBK1 and subsequent activation of IRF3/7 and NF-κB, leading to the production of interferons (IFNs) and inflammatory cytokines (7–9). Type I and III IFNs initiate an antiviral state through activating the JAK/STAT signaling pathway that induces the transcription of hundreds of IFN-stimulated genes (ISGs) (10–12). It is well known that host innate immune responses must be tightly controlled to eliminate the invading pathogens while avoiding deleterious immunopathological outcomes (13–15). However, the underlying mechanisms accounting for precise control of host innate immunity and immune homeostasis remain ambiguous and warrant further investigations.

The spleen tyrosine kinase (Syk) is a nonreceptor tyrosine kinase that mediates diverse cellular processes, including regulation of innate immune signaling (16). Notably, the role of Syk in innate immune response is highly context dependent. For instance, Syk participates in enhancing IFN-α-induced STAT1 activation in IFN-γ-primed macrophages (17). Moreover, Syk is a key component of antifungal defense mediated by dectin-1 and dectin-2, critical PRRs for fungi (18, 19). These investigations suggest a functional involvement of Syk in potentiating the antimicrobial immune response. In contrast, Syk is activated by plasmacytoid dendritic cell (pDC) regulatory receptors such as BDCA-2 and ILT7 and inhibits type I IFN response in pDC (20, 21). Additionally, Syk has been reported to phosphorylate MyD88 and TRIF, leading to Cbl-b-mediated degradation of MyD88 and TRIF and subsequent downregulation of TLR signaling (22). Syk could be activated by double-stranded RNA (dsRNA) stimulation, and silencing Syk enhances the secretion of IFN-β in murine astrocytes (23). Interestingly, a recent study has shown that gain-of-function variants in Syk result in immune deficiency and systemic inflammatory disease in humans (24). Furthermore, it is thought that Syk limits HIV-1 replication in immature monocyte-derived dendritic cells (IM-MDDCs) but promotes virus infection in primary human $CD4^+$ T cells, leading to transfer of HIV-1 from IM-MDDCs to $CD4^+$ T cells (25). These observations demonstrate that Syk exhibits distinct roles under different physiological circumstances and propose Syk as a key regulator of host innate immunity against pathogen invasion.

Our previous study revealed that Syk is critical for the activation of STAT1 at the early stage of IAV infection, which is crucial for initial antiviral immunity (26). However, the role of Syk in host innate immune response during the whole process of viral infection remains largely unknown. Here, our results show that Syk negatively regulates host antiviral immunity at the late stage of IAV infection, thereby facilitating IAV replication. Syk restrains IFN response during the late phase of IAV infection, as Syk deficiency leads to highly enhanced expression of type I and III IFNs and renders mice more resistant to IAV infection. Mechanistically, Syk interacts with TBK1 and modulates its phosphorylation status, thereby inhibiting TBK1 activation and repressing the production of IFNs. These findings reveal a critical role of Syk in temporally regulating host antiviral immune response and advance our understanding of complicated mechanisms underlying host innate immunity against viral invasion.

RESULTS

Syk favors IAV replication at late stage of the viral infection *in vitro* and *in vivo*. Our previous data reveal that Syk acts as a key kinase involved in STAT1 activation at the early stage of IAV infection, which is critical for initial antiviral immunity (26). However, the role of Syk in host antiviral immunity at the late stage of IAV infection and the effect on viral replication remain elusive. To probe the effect of Syk on IAV replication, we generated A549 cells stably expressing control or specific short hairpin RNAs (shRNAs) targeting Syk (Fig. 1A). Control and Syk knockdown cells then were infected with influenza virus A/WSN/33 (H1N1) for 16 h, and the viral loads were determined by plaque-forming assay (PFA). Unexpectedly, decreased IAV titers were observed in Syk knockdown A549 cells compared with those in control cells (Fig. 1B), indicating that disruption of Syk expression inhibited IAV replication. To further confirm the effect of Syk depletion on IAV replication, we generated Syk knockout A549 cells and examined viral replication in the cells infected with IAV at multiplicities of infection (MOIs) of 0.5 and 0.1, respectively. As shown in Fig. 1C and D, loss

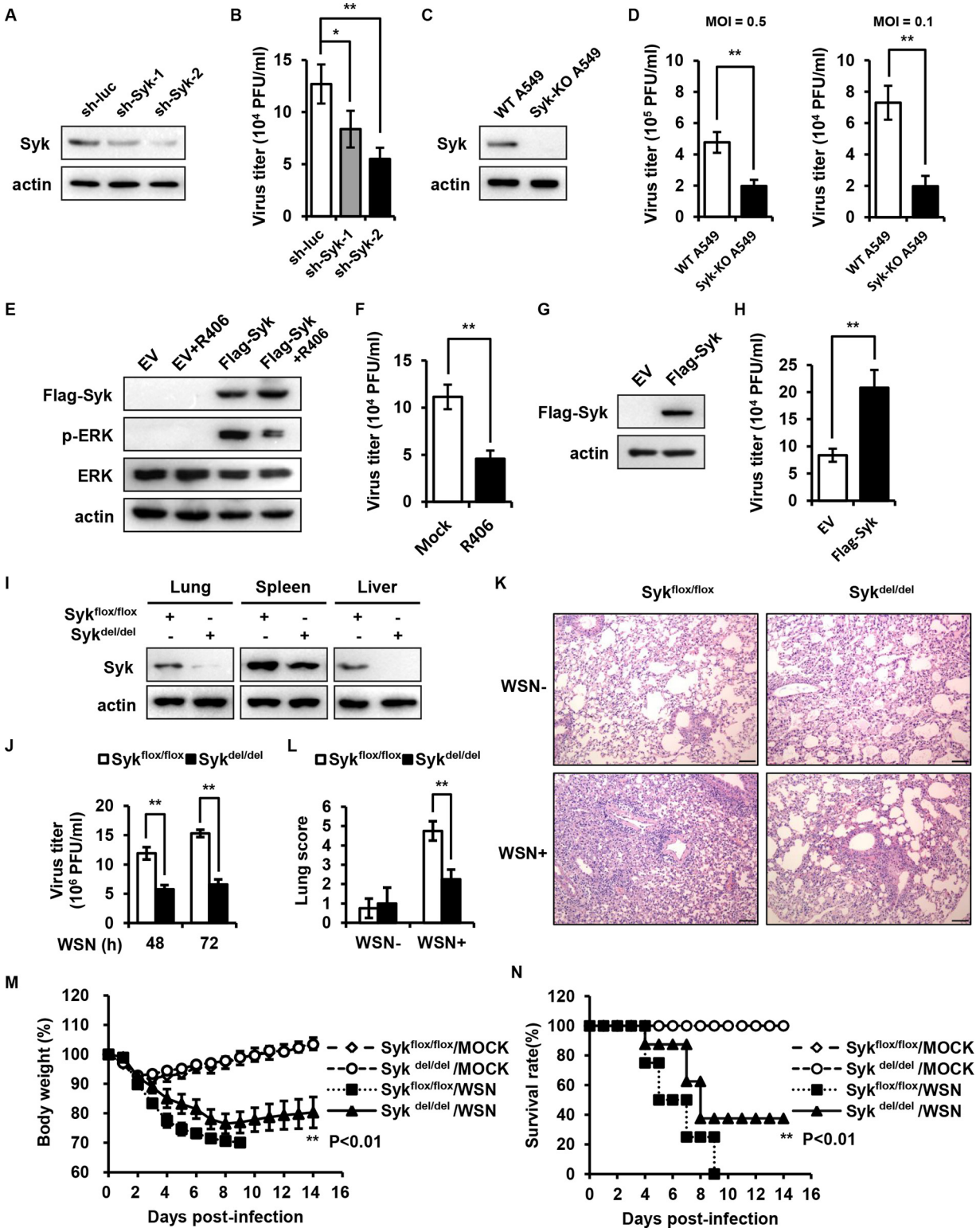

FIG 1 Syk favors IAV replication at late stage of the viral infection *in vitro* and *in vivo*. (A) Syk protein levels in A549 cells stably expressing control or Syk shRNAs were examined by Western blotting. (B) Control and Syk knockdown A549 cells were infected with influenza virus A/WSN/33 (MOI of 0.1) for 16 h, and the supernatants were collected for plaque-forming assay. (C) Syk protein levels in A549 cells stably expressing control or Syk sgRNA were detected by Western blotting. (D) Control and Syk knockout A549 cells were infected with influenza virus A/WSN/33 (MOI of 0.5 or 0.1 as indicated) for 16 h, and the supernatants were collected for plaque-forming assay. (E) HEK293T were transfected with empty vector (EV) or Flag-Syk and then mock treated or treated with R406. The phosphorylation levels of ERK were determined by Western blotting. (F) A549 cells were pretreated with DMSO or R406 (1 μM) for 30 min and then infected with WSN (MOI of 0.1) for 16 h. The supernatants were collected for plaque-forming assay. (G and H) Western blot analysis of Syk protein levels in A549 cells

(Continued on next page)

of Syk attenuated IAV replication in the cells, and the results with the different MOIs were consistent. In addition, we treated cells with the Syk inhibitor and examined IAV replication. The experiments demonstrated that treatment with the Syk inhibitor R406 impaired IAV replication in A549 cells (Fig. 1E and F), suggesting that the activation of Syk is required for efficient IAV replication. On the other hand, we also evaluated the effect of Syk overexpression on IAV replication. We found that forced expression of Syk promoted viral replication in A549 cells (Fig. 1G and H). These results indicate that Syk promotes IAV replication *in vitro*.

To further substantiate the physiological function of Syk during IAV infection *in vivo*, we employed Syk conditional knockout mice, as the germ line knockout of Syk is lethal (27). $Syk^{flox/flox}$ mice were crossed with transgenic UBC-$CreER^{T2}$ mice. Hybrid $Syk^{flox/flox}$/UBC-$CreER^{T2}$ mice were treated with tamoxifen to induce the expression of Cre recombinase, which mediated the consequent knockout of Syk. As shown in Fig. 1I, Syk protein was almost undetectable in the lungs and livers of $Syk^{flox/flox}$/UBC-$CreER^{T2}$ mice treated with tamoxifen ($Syk^{del/del}$), while a poor knockout efficiency was observed in the spleens of $Syk^{del/del}$ mice. The mice were then infected with influenza virus A/WSN/33 (H1N1) for indicated times, and viral replication was evaluated. Similar to the results obtained from *in vitro* experiments, decreased virus titers were detected in the lungs from $Syk^{del/del}$ mice. Consequently, a lower degree of lung injury caused by viral infection was observed in $Syk^{del/del}$ mice compared with that in control mice (Fig. 1J to L). Accordingly, a time course study showed that Syk knockout mice had slower body weight loss and better survival than control mice challenged with the IAV (Fig. 1M and N), implying that depletion of Syk renders mice more resistant to influenza virus infection. Together, these results suggest that Syk facilitates IAV pathogenesis *in vitro* and *in vivo*.

Syk restrains type I and III IFN responses during IAV infection. Type I and III IFNs play central roles in restricting viral replication, including IAV, and this prompted us to investigate whether Syk promotes IAV replication through regulating IFN response during the viral infection. To test this, we examined the levels of type I and III IFNs in control and Syk knockdown cells or in cells treated with or without the Syk inhibitor followed by IAV infection. We found that disruption of Syk expression or blockade of Syk activation led to a significant increase in expression of type I IFNs (IFN-α and IFN-β) upon IAV infection in A549 and THP-1 cells (Fig. 2A to E). Consistent with this, higher levels of IFN-α and IFN-β were observed in the lungs of Syk knockout mice compared with those in control mice after IAV infection (Fig. 2F and G). In addition, enhanced expression of type III IFNs (interleukin-28A/B [IL-28A/B] and IL-29) was detected in Syk-depleted A549 cells and lungs derived from Syk knockout mice after IAV infection (Fig. 2H to J). These results show that loss of Syk leads to the enhancement of type I and III IFNs expression during IAV infection, which may explain the inhibited IAV replication in Syk-depleted cells and mice.

Furthermore, we generated Syk knockout A549 cells reconstituted with either wild-type (WT) Syk, Syk mutant (Y352D), or empty vector and examined the levels of IFNs after IAV infection (Fig. 3A). As shown in Fig. 3B to F, depletion of Syk led to significantly increased expression of type I and III IFNs, while reduced levels of IFNs were observed in the Syk knockout cells reexpressing WT Syk or Syk mutant (Y352D) compared with that in Syk knockout cells, indicating that reintroduction of Syk reversed the increased expression of IFNs caused by the Syk depletion.

To further address the function of IFNs in Syk-mediated regulation of IAV replication, we generated control and IFN alpha and beta receptor subunit 1 (IFNAR1) knockout A549 cells overexpressing empty vector or Syk (Fig. 3G). The cells were then infected with IAV, and viral

FIG 1 Legend (Continued)
expressing EV or Syk (G). Control and Syk-overexpressing A549 cells were infected with influenza virus A/WSN/33 (MOI of 0.1) for 16 h, and the supernatants were collected for plaque-forming assay (H). (I) $Syk^{flox/flox}$ and $Syk^{del/del}$ mice were injected intraperitoneally with tamoxifen at a dose of 100 μg/g body weight three times. Syk protein levels in indicated tissues from WT or Syk knockout mice were examined by Western blotting. (J to L) $Syk^{flox/flox}$ and $Syk^{del/del}$ mice were treated with tamoxifen as described for panel I and then inoculated intranasally with 5×10^4 PFU of WSN. (J) The viral titers in the lungs from WT and Syk knockout mice were determined by plaque-forming assay. The histopathologic changes in the lungs from WT and Syk knockout mice on 3 dpi were determined by hematoxylin-eosin staining (K) and scored for disease severity (L). Scale bar, 100 μm. (M and N) $Syk^{flox/flox}$ and $Syk^{del/del}$ mice were treated with tamoxifen as described for panel I and then inoculated intranasally with 1×10^4 PFU of WSN. The body weight loss (M) and the survival (N) were monitored. The data are presented as means $\pm$ SD from three independent experiments. *, $P < 0.05$; **, $P < 0.01$.

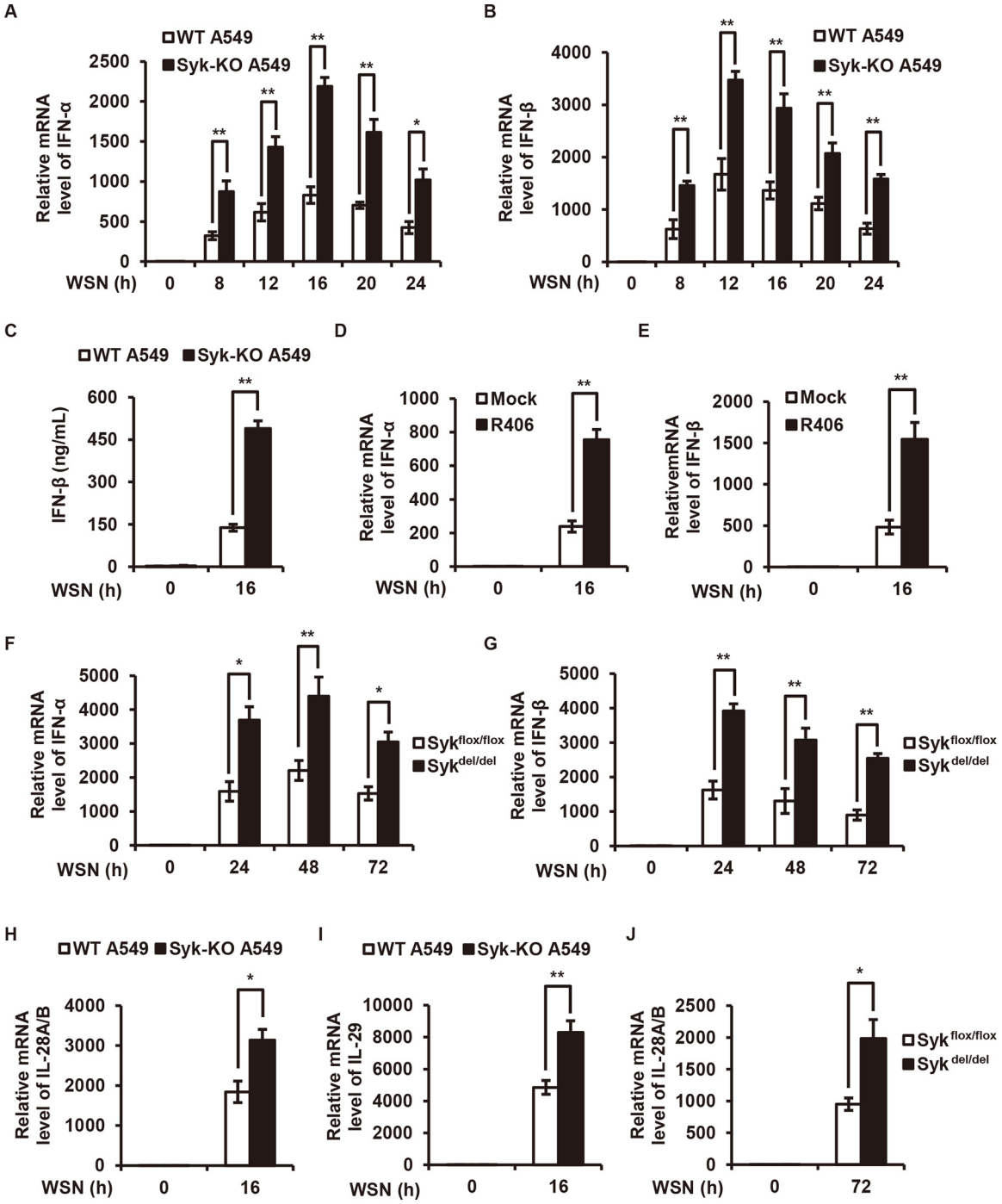

FIG 2 Syk deficiency leads to increased expression of type I and III IFNs upon IAV infection. (A and B) WT and Syk knockout (KO) A549 cells were infected with WSN (MOI of 0.5) for 0, 8, 12, 16, 20, and 24 h. The relative mRNA levels of IFN-α (A) or IFN-β (B) were examined by qRT-PCR. (C) WT and Syk knockout A549 cells were infected with WSN (MOI of 0.5) for 16 h. IFN-β protein levels in the supernatants were examined by ELISA. (D and E) THP-1 cells were pretreated with DMSO or R406 (1 μM) for 30 min, and then infected with WSN (MOI of 0.5) for 16 h. The relative mRNA levels of IFN-α (D) or IFN-β (E) were examined by qRT-PCR. (F and G) Tamoxifen-treated $Syk^{flox/flox}$ and $Syk^{del/del}$ mice were infected with 5×10^4 PFU of WSN for 0, 24, 48, and 72 h. The relative mRNA levels of IFN-α (F) or IFN-β (G) in the lungs of mice were determined by qRT-PCR. (H and I) WT and Syk knockout A549 cells were infected with WSN (MOI of 0.5) for 16 h. The relative mRNA levels of IL-28A/B (H) or IL-29 (I) were examined by qRT-PCR. (J) Tamoxifen-treated $Syk^{flox/flox}$ and $Syk^{del/del}$ mice were infected with 5×10^4 PFU of WSN for 72 h. The relative mRNA levels of IL-28A/B in the lungs of mice were examined by qRT-PCR. The data are presented as means $\pm$ SD from three independent experiments. *, $P < 0.05$; **, $P < 0.01$.

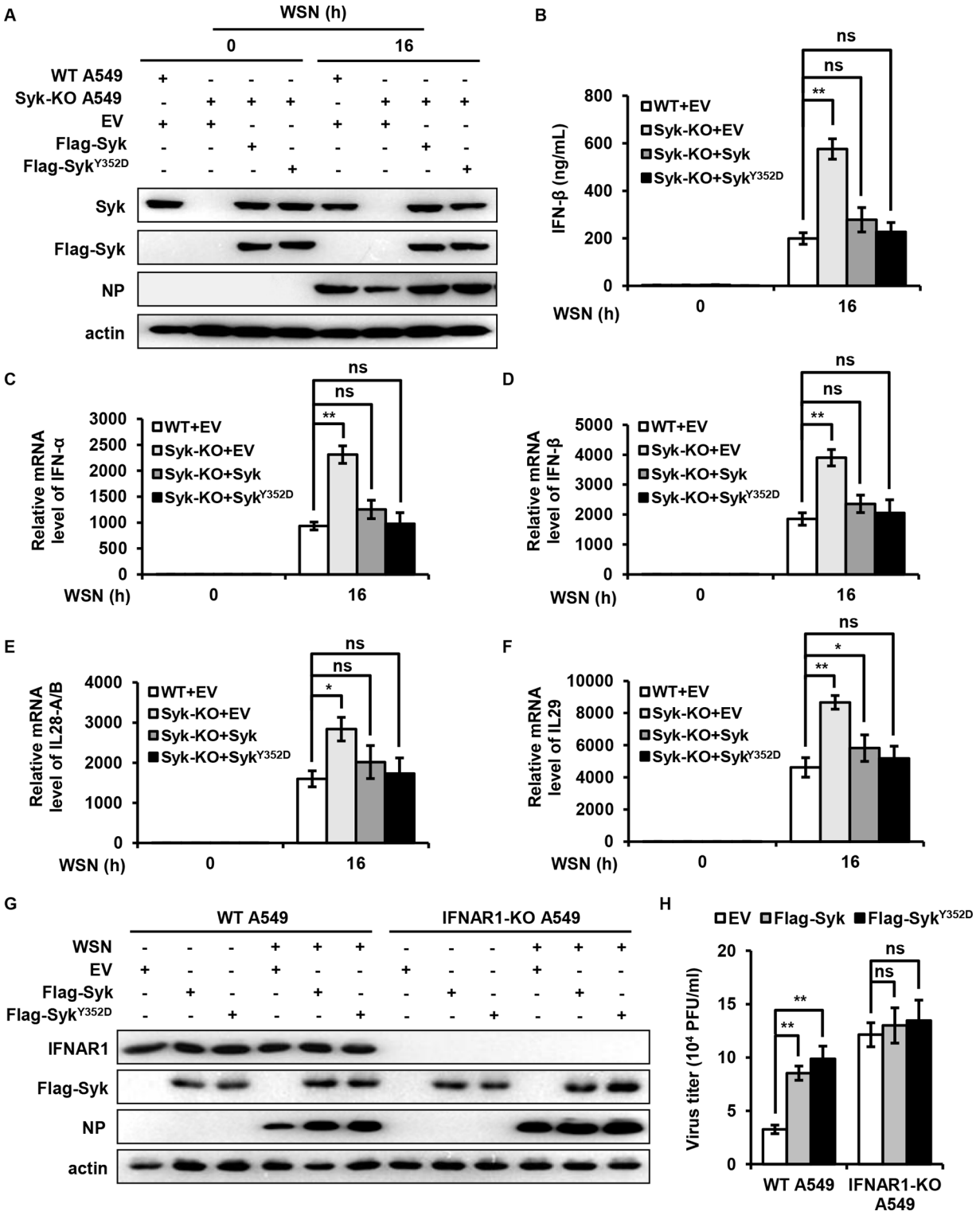

FIG 3 Syk suppresses the expression of type I and III IFNs during IAV infection. (A to F) WT and Syk knockout A549 cells were infected with retroviruses expressing EV, WT Syk, or Syk mutant (Y352D). (A) The cells were then infected with WSN (MOI of 0.5) for 16 h. Syk protein levels in these cells were detected by Western blotting. (B) The protein levels of IFN-β were determined by ELISA. The mRNA levels of IFN-α (C), IFN-β (D), IL-28A/B (E), and IL-29 (F) were examined by qRT-PCR. (G) WT and IFNAR1 knockout (KO) A549 cells were infected with retroviruses expressing EV, WT Syk, or Syk mutant (Y352D). The cells were then infected with WSN (MOI of 0.01) for 16 h. (H) The supernatants were collected for plaque-forming assay. The data are presented as means ± SD from three independent experiments. ns, not significant; *, $P < 0.05$; **, $P < 0.01$.

replication was evaluated by PFA. As shown in Fig. 3H, higher virus titers were detected in WT A549 cells overexpressing Syk compared with that in control WT cells, suggesting that Syk overexpression renders cells more susceptible to IAV infection. In contrast, comparable virus titers were observed between IFNAR1 knockout A549 cells overexpressing Syk and control IFNAR1 knockout cells, indicating that Syk-mediated promotion of IAV replication was abrogated in the absence of IFNAR1. Collectively, these observations imply that Syk promotes IAV replication through restriction of type I and III IFN responses.

Syk negatively regulates activation of STAT1 and expression of ISGs during the late stage of IAV infection. Type I and III IFNs bind to their receptors and activate JAK/STAT signaling pathway, thereby inducing the expression of hundreds of ISGs. To determine the effect of Syk on STAT1 activation during the late stage of IAV infection, we examined the levels of STAT1 phosphorylation in lungs from WT and Syk knockout mice at 24, 48, and 72 h after IAV infection. As shown in Fig. 4A, higher phosphorylation levels of STAT1 were observed in lungs derived from Syk knockout mice than those in WT mice. Alveolar epithelial cells (AECs) derived from AEC-specific Syk knockout mice or control mice then were infected with IAV, and the phosphorylation of STAT1 was examined. Similarly, the levels of STAT1 phosphorylation were significantly increased in the infected AECs deficient in Syk than those from WT mice (Fig. 4B). Since ISGs are the important downstream antiviral effectors orchestrated by the IFN/STAT1 pathway, we examined the effect of Syk on the expression of several critical ISGs at the late stage of IAV infection. As expected, we observed that disruption of Syk expression or inhibition of Syk activity led to increased expression of Mx1 and IFITM3 in A549 cells at 16 h postinfection (hpi) (Fig. 4C to E). Furthermore, higher mRNA and protein levels of Mx1 and IFITM3 were found in the lungs from Syk knockout mice than those in control mice challenged with IAV for 24, 48, and 72 h (Fig. 4F to H). In addition, AECs derived from AEC-specific Syk knockout mice or control mice were infected with IAV, and the expression of Mx1 and IFITM3 in the cells was also examined. The levels of Mx1 and IFITM3 were significantly increased in the infected AECs from AEC-specific Syk knockout mice compared to those from control animals (Fig. 4I and J). These results indicate that Syk negatively regulates the activation of STAT1 and expression of some ISGs during the late phase of IAV infection.

Syk temporally regulates host antiviral immunity during IAV infection. Our previous study showed that Syk is critical for the initial activation of STAT1 before IFN production during IAV infection (26). Unexpectedly, the present data indicate that Syk represses the expression of IFNs at late stages of IAV infection, which leads to attenuated activation of STAT1 and expression of ISGs, suggesting a dynamic role for Syk in regulating host antiviral immunity. This prompted us to assess the effect of Syk on STAT1 activation and ISG expression during the whole process of the IAV life cycle. We infected control and Syk knockout A549 cells with IAV and examined the effect of Syk depletion on STAT1 activation at different time points during IAV infection. The phosphorylation levels of STAT1 were impaired in Syk knockout cells compared with that in control cells at early time points after IAV infection (4 hpi). In contrast, enhanced STAT1 phosphorylation was observed in Syk-depleted cells compared with that in control cells at late time points (8 hpi and later) (Fig. 5A). Accordingly, the expression of Mx1 and IFITM3 was decreased in Syk knockout cells compared with that in control cells at early time points of IAV infection (4 hpi), while increased expression of these ISGs was observed in Syk-depleted cells compared with that in control cells at late time points (8 hpi and later) (Fig. 5B and C). To confirm this finding, we employed a poly(I:C) transfection assay. Control and Syk knockout A549 cells were transfected with poly(I:C). The supernatants were collected and applied to WT A549 cells. As shown in Fig. 5D, the phosphorylation levels of STAT1 in A549 cells treated with supernatant from Syk knockout cells were higher than those in A549 cells treated with supernatant from control cells. Accordingly, higher levels of Mx1 and IFITM3 were observed in A549 cells treated with supernatant from Syk knockout cells than those in A549 cells treated with supernatant from control cells. These results suggest that Syk inhibits type I IFN expression, thereby suppressing STAT1 activation and restraining host antiviral response.

To further elucidate the dynamic role for Syk in regulating host antiviral immunity *in vivo*, we infected WT and Syk knockout mice with IAV and performed a time course experiment for measurement of IFN expression during IAV infection. The expression of

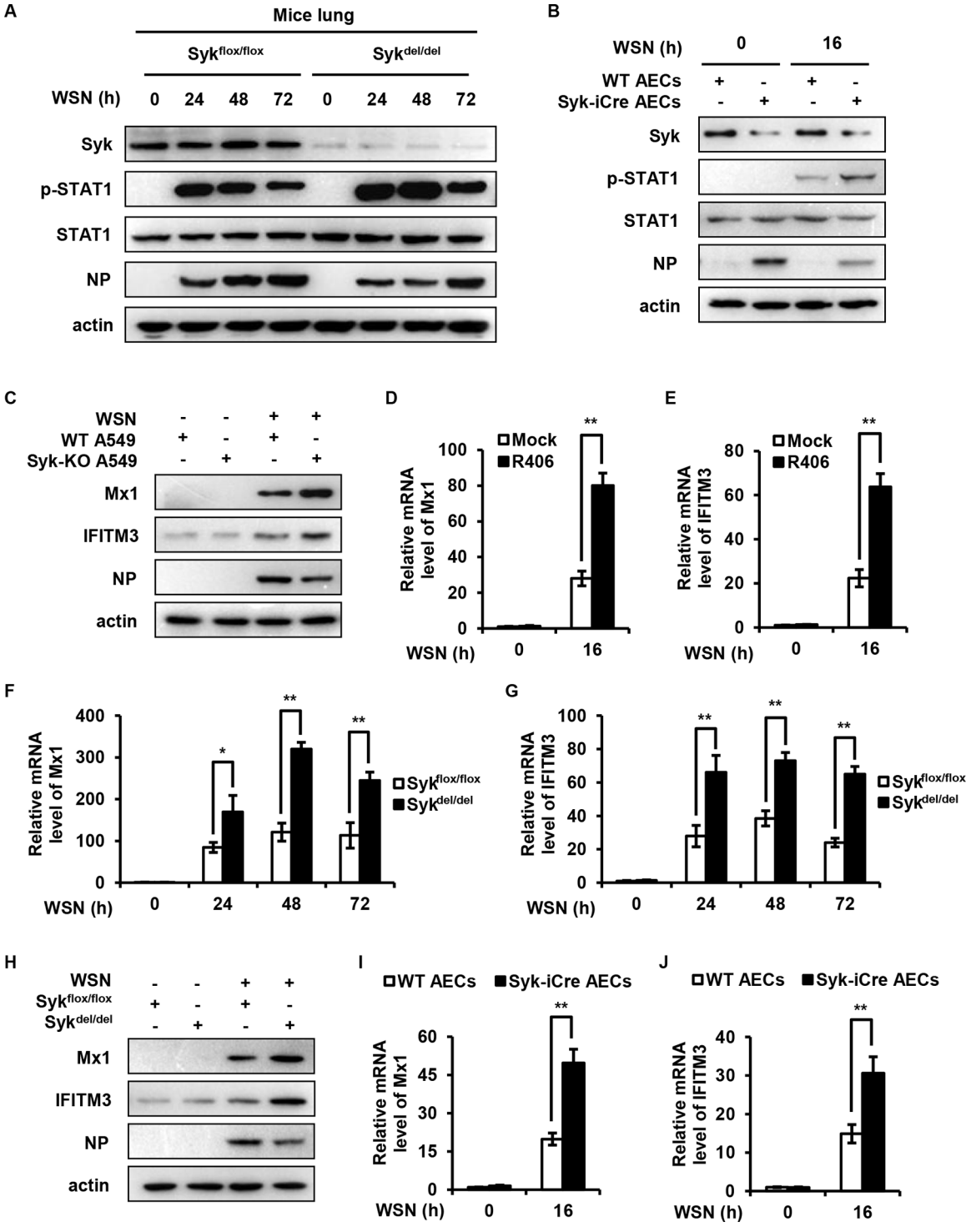

FIG 4 Syk negatively regulates the activation of STAT1 and the expression of ISGs during the late phase of IAV infection. (A) Tamoxifen-treated $Syk^{flox/flox}$ and $Syk^{del/del}$ mice were infected with 5×10^4 PFU of WSN for 0, 24, 48, and 72 h. The levels of STAT1 phosphorylation in the lungs of mice were detected by Western blotting. (B) AECs derived from Syk iCre or WT mice were infected with WSN (MOI of 0.5) for 16 h. The levels of STAT1 phosphorylation were detected by Western blotting. (C) WT and Syk knockout A549 cells were infected with WSN (MOI of 0.5) for 16 h. The protein levels of Mx1 and IFITM3 were examined by Western blotting. (D and E) THP-1 cells were pretreated with DMSO or R406 (1 μM) for 30 min, and then infected with WSN (MOI of 0.5) for 16 h. The relative mRNA levels of Mx1 (D) or IFITM3 (E) were measured by qRT-PCR. (F to H) Tamoxifen-treated $Syk^{flox/flox}$ and $Syk^{del/del}$ mice were infected with 5×10^4 PFU of WSN for 0, 24, 48, and 72 h. qRT-PCR was employed to determine the relative mRNA levels of Mx1 (F) or IFITM3 (G) in the lungs of mice. (H) The protein levels of Mx1 and IFITM3 in the lungs of mice were examined by Western blotting. (I and J) AECs derived from Syk iCre or WT mice were infected with WSN (MOI of 0.5) for 16 h. The relative mRNA levels of Mx1 (I) or IFITM3 (J) were measured by qRT-PCR. The data are presented as means $\pm$ SD from three independent experiments, *, $P < 0.05$; **, $P < 0.01$.

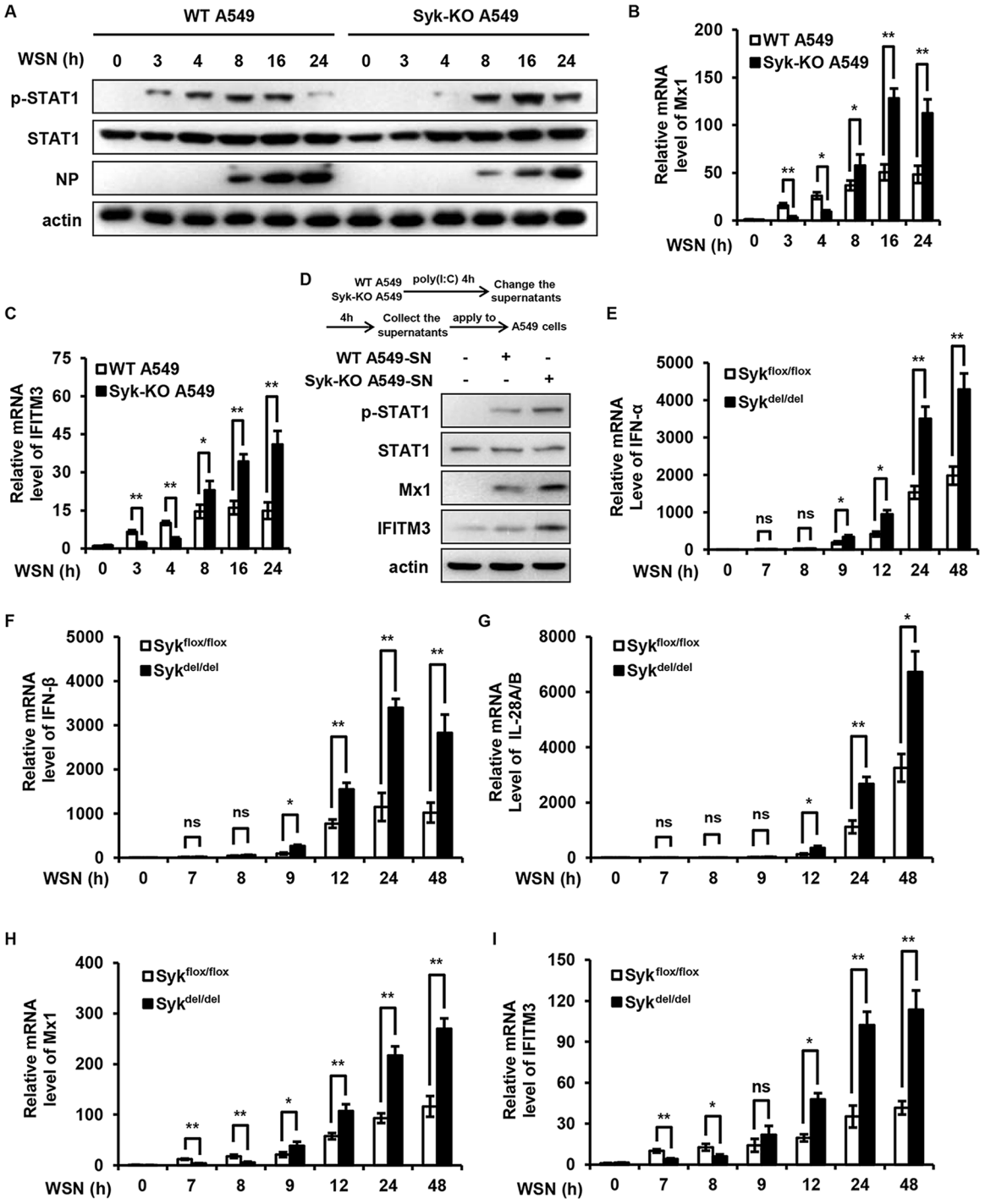

FIG 5 Syk temporally regulates host antiviral immunity during IAV infection. (A) WT and Syk knockout A549 cells were infected with WSN (MOI of 0.5) for 0, 3, 4, 8, 16, and 24 h. The levels of STAT1 phosphorylation were examined by Western blotting. (B and C) WT and Syk knockout A549 cells were infected with WSN (MOI of 0.5) for 0, 3, 4, 8, 16, and 24 h. The relative mRNA levels of Mx1 (B) or IFITM3 (C) were examined by qRT-PCR. (D) WT and Syk knockout A549 cells were transfected with poly(I:C). The supernatants were collected and applied to WT A549 cells. The phosphorylation levels of STAT1, and protein levels of Mx1 and IFITM3 were detected by Western blotting. (E to I) Tamoxifen-treated $Syk^{flox/flox}$ and $Syk^{del/del}$ mice were infected with 5×10^4 PFU of WSN for 0, 7, 8, 9, 12, 24, 48 h. qRT-PCR was employed to determine the mRNA levels of IFN-α (E), IFN-β (F), IL28A/B (G), Mx1(H), or IFITM3 (I) in the lungs of mice. The data are presented as means ± SD from three independent experiments. *, $P < 0.05$; **, $P < 0.01$.

type I IFNs (IFN-α and IFN-β, 8 hpi) and type III IFN (IL-28A/B, 9 hpi) was not detectable in WT and Syk knockout mice at early time points after IAV infection, while enhanced expression of IFN-α, IFN-β, and IL-28A/B was observed in the lungs of Syk knockout mice compared with that in WT mice at late time points after IAV infection (12 hpi and

later) (Fig. 5E to G). Accordingly, expression of Mx1 and IFITM3 was impaired in the lungs of Syk knockout mice compared with that in WT mice at early time points of IAV infection (8 hpi). In contrast, increased expression of Mx1 and IFITM3 was observed in the lungs from Syk knockout mice compared to that in WT mice at late time points (12 hpi and later) (Fig. 5H and I). Collectively, these observations suggest that Syk is involved in temporally regulating host innate immune signaling. At the early stage of the viral infection, Syk was employed by the host to mediate the activation of STAT1 and initiate rapid antiviral immunity, thereby defending against the virus. In contrast, Syk might be hijacked by the virus at late infection stages to antagonize the antiviral response mediated by IFNs. There is also the possibility that Syk is manipulated by the host to avoid excessive activation of innate immune responses.

Syk promotes SeV, HSV, and PRV replication *in vitro* by suppressing type I IFN response. Next, we investigated whether Syk regulates IFN response initiated by a broad spectrum of viruses. We performed infection experiments using various viruses, including Sendai virus (SeV), herpes simplex virus (HSV), pseudorabies virus (PRV), and Muscovy duck reovirus (MDRV). Interestingly, we found that disruption of Syk expression or inhibition of Syk activity led to increased expression of IFN-β and ISGs (ISG56, Mx1, and ISG15) and enhanced phosphorylation of STAT1 induced by infection with SeV, HSV, or PRV (Fig. 6A to F). As expected, disruption of Syk expression or inhibition of Syk activity resulted in reduced viral gene replication, including SeV-NP, HSV-GC, and PRV-gE (Fig. 6A to F), indicating that Syk suppressed the type I IFN response, thereby promoting SeV, HSV, or PRV replication. However, blocking the activity of Syk had no significant effect on IFN-β production, Mx1 expression, STAT1 activation, and virus replication in response to MDRV infection (Fig. 6G and H). These results suggest that Syk represses type I IFN response induced by some viruses, such as IAV, SeV, HSV, and PRV, thereby facilitating virus replication.

Syk impairs TBK1 activation during IAV infection. Next, we proceeded to decode the mechanism whereby Syk restrains IFN response during IAV infection. First, we determined whether Syk suppresses RLR-dependent signaling. Thus, 293T cells were transfected with IFN-β luciferase reporter and either RIG-I, MAVS, TBK1, IRF3(5D), or p65 expression plasmid together with EV or Syk plasmid. The luciferase assay showed that Syk inhibited RIG-I-, MAVS-, and TBK1-mediated IFN-β luciferase activation but not IRF3(5D)- or p65-induced IFN-β luciferase activation (Fig. 7A), implying that Syk restrains RLR signaling at the TBK1 level. We also evaluated whether Syk functions similarly when TBK1 is activated by other adaptor proteins (STING and TRIF). Indeed, Syk also inhibited TRIF- and cGAS/STING-mediated IFN-β luciferase activation (Fig. 7A). In addition, we assessed whether Syk affected the activation of NF-κB and found that Syk had no significant effect on the NF-κB activity in response to IAV infection (data not shown). Notably, it has been shown that Src kinase-mediated tyrosine phosphorylation of TBK1 prevents TBK1 activation and suppresses innate antiviral responses (28). This prompted us to evaluate whether Syk regulates the activation of TBK1 and consequent production of IFNs through enhancing the tyrosine phosphorylation of TBK1. To test this, we first examined the association of Syk with TBK1. We transfected Flag-tagged Syk into HEK293T cells and performed immunoprecipitation (IP) assays. As shown in Fig. 7B, IP of Flag-Syk effectively brought down TBK1, suggesting the interaction between Syk and TBK1. Interestingly, a previous study has reported that Syk interacts with TBK1, TRAF3, TRAF6, and TAK1 and plays an important role in TLR4-mediated signaling (29). We then determined whether Syk could regulate phosphorylation of TBK1 protein. We expressed the WT and a constitutively active mutant of Syk (Y352D) in 293T cells and examined tyrosine phosphorylation levels of TBK1. As shown in Fig. 7C, forced expression of WT Syk leads to a significantly increased tyrosine phosphorylation of TBK1, while a much higher phosphorylation level of TBK1 was observed in the cells expressing the Syk Y352D mutant, indicating that Syk is associated with tyrosine phosphorylation of TBK1. Furthermore, we examined the effect of Syk on TBK1 activation. HEK293T cells were cotransfected with TBK1 plasmid and either EV or Syk plasmid. At 24 h posttransfection, cells were analyzed for TBK1 activation. We observed that Syk inhibited phosphorylation of TBK1 Ser 172 and IRF3 in a dose-dependent manner (Fig. 7D). These results indicate that Syk interacts with TBK1 and modulates its serine and tyrosine phosphorylation, thereby impeding TBK1 activation.

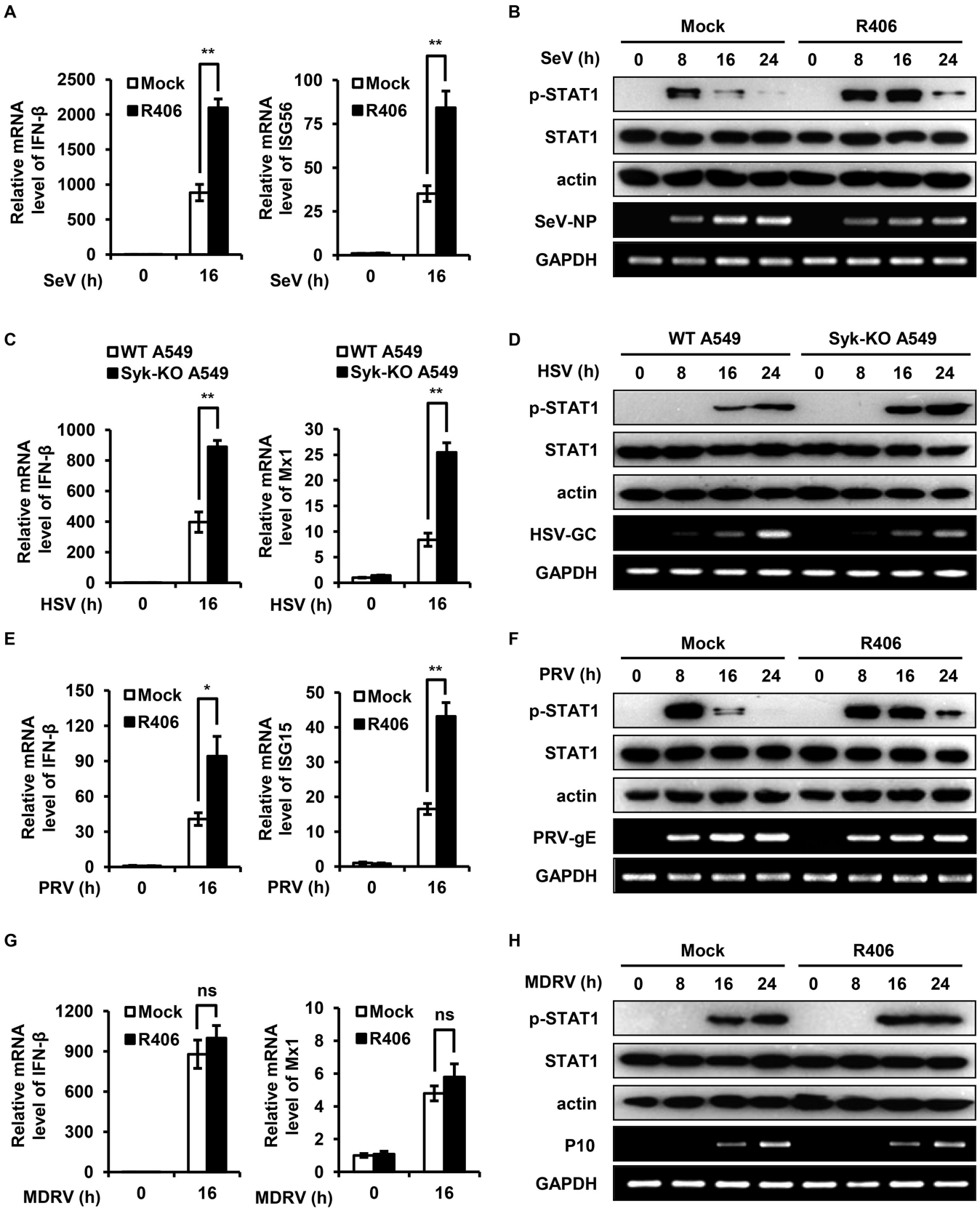

FIG 6 Syk promotes SeV, HSV, and PRV replication *in vitro* by suppressing type I IFN response. (A and B) HEK293T cells were pretreated with DMSO or R406 (1 μM) for 30 min and then infected with SeV for 0, 8, 16, and 24 h. (A) The relative mRNA levels of IFN-β and ISG56 were examined by qRT-PCR. (B) The levels of STAT1 phosphorylation were detected by Western blotting. (C and D) WT and Syk knockout A549 cells were infected with HSV for 0, 8, 16, and 24 h.

(Continued on next page)

Next, we evaluated the effect of Syk on TBK1 activation upon IAV infection. We observed that disruption of Syk expression or inhibition of Syk activation led to a significant increase of the serine phosphorylation of TBK1 in A549 and THP-1 cells, respectively (Fig. 7E and F). Conversely, ectopic expression of Syk profoundly reduced the serine phosphorylation levels of TBK1 following infection with IAV (Fig. 7G). Collectively, these results suggest that Syk impedes TBK1 activation likely through enhancing the tyrosine phosphorylation of TBK1 during IAV infection.

DISCUSSION

Our previous study has revealed that Syk-mediated STAT1 activation before the production of IFNs is critical for initial antiviral immunity (26). However, the role of Syk in host antiviral immune response during the late phase of IAV infection and the effect on viral replication remain obscure. In the present study, we found that Syk negatively regulates antiviral immune response at the late stage of IAV infection and facilitates viral replication. Syk deficiency led to enhanced expression of type I and III IFNs during IAV infection, thereby suppressing IAV replication and rendering mice more resistant to IAV infection. Mechanistically, Syk interacted with TBK1 and mediated its phosphorylation status, thereby suppressing TBK1 activation and restraining the IFN response. These observations indicate that Syk participates in the initiation of rapid antiviral immune defense at the early stage of virus infection while it restrains innate immune response at the late stage of IAV infection, suggesting a critical role of Syk in temporally regulating host antiviral immunity.

Host innate immune responses are essential for eliminating invading pathogens. However, excessive activation of the immune response leads to autoimmune or inflammatory diseases (13). The overwhelming immune response induced by highly pathogenic IAV, known as cytokine storm, can lead to life-threatening tissue damage (30–32). Therefore, it is of vital importance to precisely regulate the host immune response. An increasing number of host factors that fine-tune antiviral immunity have been identified (33–37). For example, TRIM38 plays an essential role in the early phase of host defense against RNA and DNA viruses through enhancing sumoylation of RIG-I/MDA5 and cGAS/STING, respectively, thereby initiating antiviral immune response (38, 39), whereas it negatively regulates TLR and RIG-I signaling by promoting the degradation of NAP1, TRAF6, and TRIF (40–42). In addition, TRIM8 prevents phosphorylated IRF7 from degradation and triggers virus-induced IFN response in human plasmacytoid dendritic cells (pDCs), while it also contributes to the termination of TLR3/4-mediated inflammatory and innate immune responses by disrupting TRIF-TBK1 interaction (43, 44). Moreover, RNF26 protects MITA (also called STING) from degradation at the early stage of viral infection, whereas it promotes the degradation of IRF3 in the late phase of viral infection (45), indicating that RNF26 temporally regulates innate antiviral response. Despite this progress, underlying mechanisms accounting for stringent control of host innate immune response are still not fully elucidated. Notably, Syk has recently come forth as an important modulator of immune signaling, but different functional consequences of Syk in innate immunity have been exhibited, which may be attributed to the type of pathogen and cell/tissue and the phase of infection. Syk is well known for its ability to induce inflammation (46). Nevertheless, recent studies have demonstrated that Syk also participates in the negative regulation of inflammatory responses. Syk-deficient macrophages secrete more proinflammatory cytokines than wild-type macrophages in response to lipopolysaccharide, CpG DNA, and synthetic lipopeptide (47). In addition, upon infection with porcine reproductive and respiratory syndrome virus (PRRSV) or vesicular stomatitis virus (VSV), silencing Syk leads to increased transcription of proinflammatory cytokines (48). Moreover, Syk inhibits TLR-induced IFN production

FIG 6 Legend (Continued)
The relative mRNA levels of IFN-β and Mx1 (C) and STAT1 phosphorylation (D) were examined by qRT-PCR and Western blotting, respectively. (E and F) PK15 cells were pretreated with DMSO or R406 (1 μM) for 30 min and then infected with PRV for 0, 8, 16, and 24 h. (E) The relative mRNA levels of IFN-β and ISG15 were examined by qRT-PCR. (F) The levels of STAT1 phosphorylation were detected by Western blotting. (G and H) HEK293T cells were pretreated with DMSO or R406 (1 μM) for 30 min and then infected with MDRV for 0, 8, 16, and 24 h. The relative mRNA levels of IFN-β and Mx1 (G) and STAT1 phosphorylation (H) were examined by qRT-PCR and Western blotting, respectively. The data are presented as means $\pm$ SD from three independent experiments. ns, not significant; *, $P < 0.05$; **, $P < 0.01$.

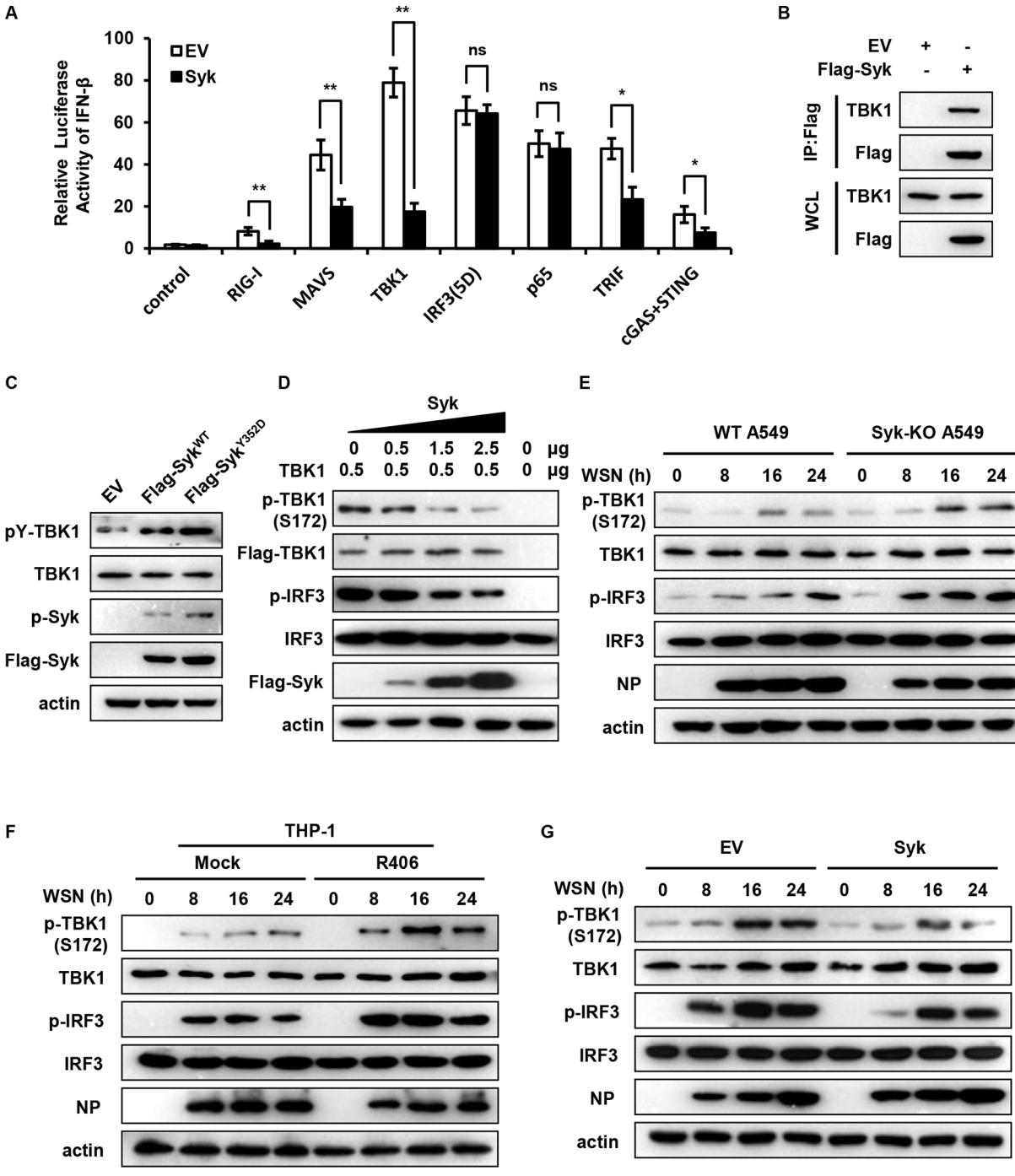

FIG 7 Syk impairs TBK1 activation during IAV infection. (A) HEK293T cells were transfected with the IFN-β luciferase reporter and the RIG-I, MAVS, TBK1, IRF3 (5D), p65, TRIF, or cGAS and STING expression plasmid together with EV or Syk. Twenty-four hours after transfection, the cells were harvested for luciferase assay. (B) HEK293T cells were transfected with EV or Flag-Syk followed by immunoprecipitation (IP) using Flag antibody. The IP and input lysates were subjected to Western blotting and probed with the indicated antibodies. WCL, whole-cell lysate. (C) HEK293T cells were transfected with EV, WT Syk, or Syk mutant (Y352D). The tyrosine phosphorylation levels of TBK1 were determined by Western blotting. (D) HEK293T cells were cotransfected with one plasmid expressing TBK1 and various amounts of plasmids encoding Syk. At 24 hpt, cells were analyzed for TBK1 and IRF3 phosphorylation by Western blotting. (E) WT and Syk knockout A549 cells were infected with WSN (MOI of 0.5) for 0, 8, 16, and 24 h. The phosphorylation levels of TBK1 and IRF3 in cells were examined by Western blotting. (F) THP-1 cells were pretreated with DMSO or R406 (1 μM) for 30 min and then infected with WSN (MOI of 0.5) for 0, 8, 16, and 24 h. The phosphorylation levels of TBK1 and IRF3 in cells were detected by Western blotting. (G) Control and Syk-overexpressing A549 cells were infected with WSN (MOI of 0.5) for 0, 8, 16, and 24 h. The phosphorylation levels of TBK1 and IRF3 in cells were examined by Western blotting. The data are presented as means $\pm$ SD from three independent experiments. ns, not significant; *, $P < 0.05$; **, $P < 0.01$.

in human pDCs stimulated by influenza virus or murine astrocytes following stimulation with viral dsRNA mimetics (20, 21, 23). However, the role of Syk in host antiviral immune response during the life cycle of IAV in pulmonary epithelial cells and the effects on viral replication are not yet clear.

Our group has previously shown that STAT1 activation mediated by Syk rather than the cytokine-activated JAK signaling at the initial stage of viral infection is important for establishing antiviral immunity at the beginning of IAV infection (26). Unexpectedly, the present work reveals that Syk restrains type I and III IFN responses at late stages of IAV infection, indicating that Syk has a dynamic role in the regulation of host immune response. It has been shown that the life cycle of influenza virus *in vitro* is about 4 to 6 h, and the early stage and late stage of IAV infection are defined *in vitro* (49, 50). We performed the time course experiments *in vitro* and *in vivo* for functional analysis of Syk and measurement of IFN expression in IAV-infected host with the WT and deficiency or inactivation of Syk. The increased expression of IFNs was not detectable until 8 hpi in infected mice, which we call the early stage of IAV infection *in vivo*, at which stage we observed that expression of Mx1 and IFITM3 was impaired in the infected lungs of Syk knockout mice compared with that in WT mice (26). Nevertheless, no apparent manifestations caused by IAV infection, such as body weight loss and death, were observed until 2 days postinfection (dpi) in mice challenged with IAV compared with uninfected mice under our conditions. This is likely because molecular changes occur prior to the development of physical symptoms. Therefore, it is difficult to probe the effect of Syk deficiency on physical symptoms and viral pathogenesis at the early stage of IAV infection *in vivo*. In contrast, expression of IFNs in mice was significantly induced by IAV at 24 hpi and later, which we call the late stage of IAV infection *in vivo*. We found that expression of IFNs, Mx1, and IFITM3 was significantly enhanced in the lungs of Syk knockout mice compared with that in WT mice at the late stage of IAV infection. Accordingly, Syk knockout mice displayed slower body weight loss and better survival than WT mice at 3 dpi and later after IAV infection. These observations suggest that Syk is involved in temporally regulating host innate immune responses. At the early stage of IAV infection, Syk was employed by the host to mediate the activation of STAT1 and initiate rapid antiviral immunity before virus-induced production of IFNs, thereby defending against the infection. In contrast, after the production of IFNs and inflammatory cytokines at the late stage of viral infection, Syk may be manipulated by the host to avoid excessive activation of innate immune and inflammatory responses and to protect the host. There is also another possibility that Syk is hijacked by the virus to antagonize the antiviral IFN response after the production of IFNs and to survive in the host. It is of interest to evaluate the effect of Syk on the inflammatory response during viral infection in the future. In addition, we utilized the lowly pathogenic IAV strain (A/WSN/1933) in the current study. The effects of Syk on host innate immunity in response to highly pathogenic IAV infection remains unknown. The pathological progression induced by highly pathogenic IAV infection is more rapid and severe, which may compel the host to prime immediate antiviral responses to defend against such infection. Under this circumstance, Syk-mediated initial antiviral response at the early stage of IAV infection might be employed by the host to combat the viral infection. Further studies are needed to elucidate precise mechanisms underlying the fine-tuning of Syk-mediated temporal regulation of host innate immunity and to evaluate the clinical significance of Syk-involved immune response in the future.

In an attempt to decode mechanisms underlying Syk-mediated suppression of IFN response during IAV infection, we determined that Syk elicited its inhibitory effect on RLR signaling through modulation of TBK1. We found that forced expression of Syk causes enhanced tyrosine phosphorylation of TBK1, which is accompanied by decreased serine phosphorylation and impaired activation of TBK1, indicating that Syk impedes TBK1 activation through promoting tyrosine phosphorylation of TBK1. This is consistent with the previous study that tyrosine phosphorylation of TBK1 prevents the serine phosphorylation of TBK1 at Ser172, thereby disrupting TBK1 dimerization and activation (28). In addition, we observed that Syk-mediated promotion of IAV replication was abolished in TBK1 knockdown cells (data not shown), suggesting that Syk regulates IAV replication in a TBK1-dependent

manner. On the other hand, our previous work has shown that Syk interacts with MAVS and is activated by RIG-I/MAVS signaling upon IAV infection. However, whether TBK1 is involved in the regulation of Syk activation and whether they form a negative feedback loop during IAV infection remains to be determined. Moreover, the precise mechanisms underlying the switch of Syk function in host antiviral immunity during viral infection warrant further studies.

Together with our previous data, these findings show that Syk facilitates IAV replication through suppression of innate immune response at the late stage of viral infection and reveal a critical role of Syk in temporally regulating host innate immunity. The translational potential of the Syk inhibitor for treatment of IAV infections and immune disorders deserves further investigations.

MATERIALS AND METHODS

Ethics statement. All animal experiments were approved by the Research Ethics Committee of Institute of Microbiology, Chinese Academy of Sciences (permit number SQIMCAS2019033). All mouse experimental procedures were carried out in accordance with the Regulations for the Administration of Affairs Concerning Experimental Animals, approved by the State Council of People's Republic of China.

Cell lines and cell culture. A549, HEK293T, MDCK, THP-1, and PK15 cell lines were purchased from the American Type Culture Collection (ATCC) (Manassas, VA, USA). Cells were maintained in Dulbecco's modified Eagle's medium (DMEM) (Gibco, USA) or RPMI 1640 (Gibco, USA) supplemented with 10% fetal bovine serum (Gibco, USA) and antibiotics (penicillin and streptomycin; Invitrogen, Carlsbad, CA).

Viruses and viral infection. Influenza A virus A/WSN/1933 (H1N1) was provided by Dayan Wang (Chinese National Influenza Center, Beijing, China) and propagated in specific-pathogen-free (SPF) chicken embryos. HSV-1 and MDRV were kindly provided by Jinghua Yan (Institute of Microbiology, Chinese Academy of Sciences, Beijing, China) and propagated in Vero cells. SeV was propagated in SPF chicken embryos, and PRV was propagated in MDCK cells as previously described (36). WSN and HSV-1 were used to infect A549 cells. SeV and MDRV were employed to infect HEK293T cells. PRV was used to infect PK15 cells.

Antibodies and reagents. ERK, p-ERK (Thr202/Tyr204), p-STAT1 (Tyr701), p-Syk (Tyr525/526), p-IRF3 (Ser386), IRF3, p-TBK1 (Ser172), and TBK1 antibodies were purchased from Cell Signaling Technology (Danvers, MA, USA). β-Actin, STAT1, and Syk antibodies were purchased from Santa Cruz Biotechnology (Santa Cruz, CA, USA). Mx1 antibody was purchased from Abcam (Cambridge, UK). IFITM3 antibody was purchased from Proteintech (Rosemont, IL, USA). Flag antibody was purchased from Sigma-Aldrich (St. Louis, MO, USA). Antibody specific to influenza A virus NP was kindly provided by Wenjun Liu (Institute of Microbiology, Chinese Academy of Sciences, Beijing, China). Antibody to tyrosine-phosphorylated proteins, clone 4G10, was purchased from Merck (Darmstadt, Germany). Syk inhibitor R406 was purchased from Selleck Chemicals (Houston, TX, USA). Tamoxifen was purchased from Sigma-Aldrich (St. Louis, MO, USA).

Generation of overexpression and knockdown cell lines. The Syk-overexpressing cells were generated as described previously (51). The Syk knockdown cells were generated by infecting A549 cells with lentivirus expressing specific short hairpin RNA (shRNA) in pSIH-H1-GFP vector as described previously (52). The shRNA target sequences used in this study were the following: sh-Syk-1, GCAGGCCATCATCAGTCAGAA; sh-Syk-2, CGACAAAGACAAGACAGGGAA.

Generation of knockout cell lines. To knock out Syk or IFNAR1 gene in A549 cells, we utilized the CRISPR/Cas9 system. The detailed procedures were as described previously (26). The single guide RNA (sgRNA) target sites for Syk were 5′-GCTGGCATGGGTCCTGCCAC-3′ and 5′-GGTAATCTTCTGCCTCCTCC-3′. The sgRNA target sites for IFNAR1 were 5′-CTGCGGCGGCTCCCAGATGA-3′ and 5′-CCAGATGATGGTCGTCCTCC-3′.

Generation of Syk-deficient mice. The $Syk^{flox/flox}$ mice harboring two LoxP sequences were purchased from Jackson Laboratory (Bar Harbor, ME, USA). The UBC-$CreER^{T2}$ mice were obtained from Shanghai Research Center of Southern Model Organisms (Shanghai, China). The Sftpc-IRES-iCre (called iCre in this paper) mice were provided by GemPharmatech Co., Ltd. (Nanjing, China). The $Syk^{flox/flox}$ mice were crossed with the UBC-$CreER^{T2}$ mice, and the offspring were injected intraperitoneally with tamoxifen (Sigma-Aldrich, St. Louis, MO, USA) at a dose of 100 μg/g body weight three times as described previously (53). To delete Syk specifically in AECs, the $Syk^{flox/flox}$ mice were crossed with the iCre mice.

Mouse experiments. For virus infection, mice were inoculated intranasally with two different doses of influenza A virus A/WSN/1933 (H1N1) (1×10^4 or 5×10^4 PFU). At the indicated time points after viral infection, the mice were euthanized for further analysis.

Plaque-forming assay. For *in vitro* experiments, the supernatants of cell cultures were harvested at indicated time points postinfection. For *in vivo* experiments, the lungs of mice were homogenized and centrifuged at 2,000 $\times$ *g* for 10 min to obtain the supernatants. The viral titers in the supernatants were determined by plaque-forming assay using MDCK cells as described previously.

RNA preparation and quantitative PCR. Total RNA was extracted from cells or mice tissues using TRIzol reagent (Invitrogen, Carlsbad, CA, USA). cDNA was synthesized from total RNA using oligo(dT) primers and reverse transcriptase (RT; Promega, Madison, WI, USA) and then subjected to quantitative PCR using SYBR PremixEx TaqII (TaKaRa, Tokyo, Japan). For quantification, the $2^{-\Delta\Delta CT}$ method was used to calculate the relative RNA levels against glyceraldehyde-3-phosphate dehydrogenase (GAPDH).

Western blotting. Cells were lysed with radioimmunoprecipitation assay (RIPA) buffer supplemented with protease inhibitors. Cell lysates were separated by SDS-PAGE and then transferred onto a nitrocellulose membrane followed by immunoblotting with indicated antibodies.

ELISA. To quantify IFN-β production by host cells, the supernatants of cell cultures were harvested and then examined by enzyme-linked immunosorbent assay (ELISA) using the human IFN-β ELISA kit (Novus Biologicals, Littleton, CO, USA) according to the manufacturer's instruction.

Dual-luciferase assay. HEK293T cells were cotransfected with IFN-β luciferase reporter, Renilla luciferase control, and the plasmid encoding RIG-I, MAVS, TBK1, IRF3(5D), p65, TRIF, or cGAS/STING, together with empty vector or Syk. After 24 h of transfection, luciferase activity was measured using the dual-luciferase reporter assay system (Promega, USA) and a Luminoskan Ascent luminometer (Thermo Scientific, USA) according to the manufacturer's instructions. Relative luciferase activity was determined by the normalization of the firefly luciferase activity to that of Renilla luciferase.

Immunoprecipitation. Cells were harvested and lysed with 1 mL of cold lysis buffer (50 mM Tris-HCl [pH 7.5], 150 mM NaCl, 1% NP-40, 0.1% pepstatin A, 0.1% aprotinin, and 0.1% phenylmethylsulfonyl fluoride). After centrifugation at 12,000 $\times$ *g* for 5 min, we transferred the supernatant to another tube and added 30 μL magnetic beads into 900 μL of the supernatant. We mixed it well and incubated it with gentle agitation for 8 h at 4°C. We placed the tube on the magnetic rack for a few seconds and then removed the supernatant. We washed the beads 4 times with 1 mL of cold wash buffer (50 mM Tris-HCl [pH 7.5], 150 mM NaCl, 0.05% NP-40). The immunoprecipitates were suspended in Laemmli buffer and boiled for SDS-PAGE.

Statistical analysis. Comparison between groups was made using Student's *t* test. Data are represented as mean values $\pm$ SD (standard deviations) from three independent experiments. For the mouse survival study, Kaplan-Meier curves were generated and analyzed by log rank (Mantel–Cox) test. Differences were considered statistically significant when *P* values were less than 0.05 and highly significant when *P* values were less than 0.01.

ACKNOWLEDGMENTS

This work was supported by National Key Research and Development Program of China (2021YFD1800205) and National Natural Science Foundation of China (U1805231 and 32030110).

We thank all the members of Chen laboratory for helpful discussions and assistance.

REFERENCES

1. Medina RA, Garcia-Sastre A. 2011. Influenza A viruses: new research developments. Nat Rev Microbiol 9:590–603. https://doi.org/10.1038/nrmicro2613.
2. Paules C, Subbarao K. 2017. Influenza. Lancet 390:697–708. https://doi.org/10.1016/S0140-6736(17)30129-0.
3. Ghebrehewet S, MacPherson P, Ho A. 2016. Influenza. BMJ 355:i6258. https://doi.org/10.1136/bmj.i6258.
4. Iwasaki A, Pillai PS. 2014. Innate immunity to influenza virus infection. Nat Rev Immunol 14:315–328. https://doi.org/10.1038/nri3665.
5. Goubau D, Deddouche S, Reis e Sousa C. 2013. Cytosolic sensing of viruses. Immunity 38:855–869. https://doi.org/10.1016/j.immuni.2013.05.007.
6. Pulendran B, Maddur MS. 2014. Innate immune sensing and response to influenza. Curr Top Microbiol Immunol 386:23–71. https://doi.org/10.1007/82_2014_405.
7. Liu J, Qian C, Cao X. 2016. Post-translational modification control of innate immunity. Immunity 45:15–30. https://doi.org/10.1016/j.immuni.2016.06.020.
8. Zhou Y, He C, Wang L, Ge B. 2017. Post-translational regulation of antiviral innate signaling. Eur J Immunol 47:1414–1426. https://doi.org/10.1002/eji.201746959.
9. Chen K, Liu J, Cao X. 2017. Regulation of type I interferon signaling in immunity and inflammation: a comprehensive review. J Autoimmun 83:1–11. https://doi.org/10.1016/j.jaut.2017.03.008.
10. Ng CT, Mendoza JL, Garcia KC, Oldstone MB. 2016. Alpha and beta type 1 interferon signaling: passage for diverse biologic outcomes. Cell 164:349–352. https://doi.org/10.1016/j.cell.2015.12.027.
11. Mesev EV, LeDesma RA, Ploss A. 2019. Decoding type I and III interferon signalling during viral infection. Nat Microbiol 4:914–924. https://doi.org/10.1038/s41564-019-0421-x.
12. Grandvaux N, tenOever BR, Servant MJ, Hiscott J. 2002. The interferon antiviral response: from viral invasion to evasion. Curr Opin Infect Dis 15:259–267. https://doi.org/10.1097/00001432-200206000-00008.
13. Ivashkiv LB, Donlin LT. 2014. Regulation of type I interferon responses. Nat Rev Immunol 14:36–49. https://doi.org/10.1038/nri3581.
14. Mishra S, Kumar H. 2018. Balancing anti-viral innate immunity and immune homeostasis. Cell Mol Immunol 15:408–410. https://doi.org/10.1038/cmi.2017.98.
15. McNab F, Mayer-Barber K, Sher A, Wack A, O'Garra A. 2015. Type I interferons in infectious disease. Nat Rev Immunol 15:87–103. https://doi.org/10.1038/nri3787.
16. Mocsai A, Ruland J, Tybulewicz VL. 2010. The SYK tyrosine kinase: a crucial player in diverse biological functions. Nat Rev Immunol 10:387–402. https://doi.org/10.1038/nri2765.
17. Tassiulas I, Hu X, Ho H, Kashyap Y, Paik P, Hu Y, Lowell CA, Ivashkiv LB. 2004. Amplification of IFN-alpha-induced STAT1 activation and inflammatory function by Syk and ITAM-containing adaptors. Nat Immunol 5:1181–1189. https://doi.org/10.1038/ni1126.
18. Leibundgut-Landmann S, Osorio F, Brown GD, Reis e Sousa C. 2008. Stimulation of dendritic cells via the dectin-1/Syk pathway allows priming of cytotoxic T-cell responses. Blood 112:4971–4980. https://doi.org/10.1182/blood-2008-05-158469.
19. Robinson MJ, Osorio F, Rosas M, Freitas RP, Schweighoffer E, Gross O, Verbeek JS, Ruland J, Tybulewicz V, Brown GD, Moita LF, Taylor PR, Reis e Sousa C. 2009. Dectin-2 is a Syk-coupled pattern recognition receptor crucial for Th17 responses to fungal infection. J Exp Med 206:2037–2051. https://doi.org/10.1084/jem.20082818.
20. Cao W, Rosen DB, Ito T, Bover L, Bao M, Watanabe G, Yao Z, Zhang L, Lanier LL, Liu YJ. 2006. Plasmacytoid dendritic cell-specific receptor ILT7-Fc epsilonRI gamma inhibits Toll-like receptor-induced interferon production. J Exp Med 203:1399–1405. https://doi.org/10.1084/jem.20052454.
21. Rock J, Schneider E, Grun JR, Grutzkau A, Kuppers R, Schmitz J, Winkels G. 2007. CD303 (BDCA-2) signals in plasmacytoid dendritic cells via a BCR-like signalosome involving Syk, Slp65 and PLCgamma2. Eur J Immunol 37:3564–3575. https://doi.org/10.1002/eji.200737711.
22. Han C, Jin J, Xu S, Liu H, Li N, Cao X. 2010. Integrin CD11b negatively regulates TLR-triggered inflammatory responses by activating Syk and promoting degradation of MyD88 and TRIF via Cbl-b. Nat Immunol 11:734–742. https://doi.org/10.1038/ni.1908.
23. Mielcarska MB, Bossowska-Nowicka M, Gregorczyk-Zboroch KP, Wyżewski Z, Szulc-Dąbrowska L, Gieryńska M, Toka FN. 2019. Syk and Hrs regulate TLR3-mediated antiviral response in murine astrocytes. Oxid Med Cell Longev 2019:6927380. https://doi.org/10.1155/2019/6927380.
24. Wang L, Aschenbrenner D, Zeng Z, Cao X, Mayr D, Mehta M, Capitani M, Warner N, Pan J, Wang L, Li Q, Zuo T, Cohen-Kedar S, Lu J, Ardy RC, Mulder DJ, Dissanayake D, Peng K, Huang Z, Li X, Wang Y, Wang X, Li S, Bullers S, Gammage AN, Warnatz K, Schiefer A-I, Krivan G, Goda V, Kahr WHA, Lemaire M, Lu C-Y, Siddiqui I, Surette MG, Kotlarz D, Engelhardt KR, Griffin HR, Rottapel R, Decaluwe H, Laxer RM, Proietti M, Hambleton S, Elcombe S, Guo C-H, Grimbacher B, Dotan I, Ng SC, Freeman SA, Snapper SB, Klein C, Genomics England Research Consortium, et al. 2021. Gain-of-function variants in SYK cause immune dysregulation and systemic inflammation in humans and mice. Nat Genet 53:500–510. https://doi.org/10.1038/s41588-021-00803-4.

25. Gilbert C, Barat C, Cantin R, Tremblay MJ. 2007. Involvement of Src and Syk tyrosine kinases in HIV-1 transfer from dendritic cells to CD4+ T lymphocytes. J Immunol 178:2862–2871. https://doi.org/10.4049/jimmunol.178.5.2862.
26. Liu S, Liao Y, Chen B, Chen Y, Yu Z, Wei H, Zhang L, Huang S, Rothman PB, Gao GF, Chen JL. 2021. Critical role of Syk-dependent STAT1 activation in innate antiviral immunity. Cell Rep 34:108627. https://doi.org/10.1016/j.celrep.2020.108627.
27. Turner M, Mee PJ, Costello PS, Williams O, Price AA, Duddy LP, Furlong MT, Geahlen RL, Tybulewicz VL. 1995. Perinatal lethality and blocked B-cell development in mice lacking the tyrosine kinase Syk. Nature 378:298–302. https://doi.org/10.1038/378298a0.
28. Liu S, Chen S, Li X, Wu S, Zhang Q, Jin Q, Hu L, Zhou R, Yu Z, Meng F, Wang S, Huang Y, Ye S, Shen L, Xia Z, Zou J, Feng XH, Xu P. 2017. Lck/Hck/Fgr-mediated tyrosine phosphorylation negatively regulates TBK1 to restrain innate antiviral responses. Cell Host Microbe 21:754–768. https://doi.org/10.1016/j.chom.2017.05.010.
29. Lin Y, Huang D, Chu C, Lin Y, Lin W. 2013. The tyrosine kinase Syk differentially regulates Toll-like receptor signaling downstream of the adaptor molecules TRAF6 and TRAF3. Sci Signal 6:ra71. https://doi.org/10.1126/scisignal.2003973.
30. Liu Q, Zhou YH, Yang ZQ. 2016. The cytokine storm of severe influenza and development of immunomodulatory therapy. Cell Mol Immunol 13:3–10. https://doi.org/10.1038/cmi.2015.74.
31. Fajgenbaum DC, June CH. 2020. Cytokine storm. N Engl J Med 383:2255–2273. https://doi.org/10.1056/NEJMra2026131.
32. Tisoncik JR, Korth MJ, Simmons CP, Farrar J, Martin TR, Katze MG. 2012. Into the eye of the cytokine storm. Microbiol Mol Biol Rev 76:16–32. https://doi.org/10.1128/MMBR.05015-11.
33. Naik SK, Pattanaik K, Eich J, Sparr V, Hauptmann M, Kalsdorf B, Reiling N, Liedtke W, Kuebler WM, Schaible UE, Sonawane A. 2020. Differential roles of the calcium ion channel TRPV4 in host responses to Mycobacterium tuberculosis early and late in infection. iScience 23:101206. https://doi.org/10.1016/j.isci.2020.101206.
34. Hu MM, Shu HB. 2017. Multifaceted roles of TRIM38 in innate immune and inflammatory responses. Cell Mol Immunol 14:331–338. https://doi.org/10.1038/cmi.2016.66.
35. Wang Q, Pan W, Wang S, Pan C, Ning H, Huang S, Chiu SH, Chen JL. 2021. Protein tyrosine phosphatase SHP2 suppresses host innate immunity against influenza A virus by regulating EGFR-mediated signaling. J Virol 95:e02001-20. https://doi.org/10.1128/JVI.02001-20.
36. Chen Y, Hu J, Liu S, Chen B, Xiao M, Li Y, Liao Y, Rai KR, Zhao Z, Ouyang J, Pan Q, Zhang L, Huang S, Chen JL. 2021. RDUR, a lncRNA, promotes innate antiviral responses and provides feedback control of NF-kappaB activation. Front Immunol 12:672165. https://doi.org/10.3389/fimmu.2021.672165.
37. Sun T, Wei C, Wang D, Wang X, Wang J, Hu Y, Mao X. 2021. The small RNA mascRNA differentially regulates TLR-induced proinflammatory and antiviral responses. JCI Insight 6:e150833. https://doi.org/10.1172/jci.insight.150833.
38. Hu MM, Yang Q, Xie XQ, Liao CY, Lin H, Liu TT, Yin L, Shu HB. 2016. Sumoylation promotes the stability of the DNA sensor cGAS and the adaptor STING to regulate the kinetics of response to DNA virus. Immunity 45:555–569. https://doi.org/10.1016/j.immuni.2016.08.014.
39. Hu MM, Liao CY, Yang Q, Xie XQ, Shu HB. 2017. Innate immunity to RNA virus is regulated by temporal and reversible sumoylation of RIG-I and MDA5. J Exp Med 214:973–989. https://doi.org/10.1084/jem.20161015.
40. Zhao W, Wang L, Zhang M, Wang P, Yuan C, Qi J, Meng H, Gao C. 2012. Tripartite motif-containing protein 38 negatively regulates TLR3/4- and RIG-I-mediated IFN-beta production and antiviral response by targeting NAP1. J Immunol 188:5311–5318. https://doi.org/10.4049/jimmunol.1103506.
41. Zhao W, Wang L, Zhang M, Yuan C, Gao C. 2012. E3 ubiquitin ligase tripartite motif 38 negatively regulates TLR-mediated immune responses by proteasomal degradation of TNF receptor-associated factor 6 in macrophages. J Immunol 188:2567–2574. https://doi.org/10.4049/jimmunol.1103255.
42. Hu MM, Xie XQ, Yang Q, Liao CY, Ye W, Lin H, Shu HB. 2015. TRIM38 negatively regulates TLR3/4-mediated innate immune and inflammatory responses by two sequential and distinct mechanisms. J Immunol 195:4415–4425. https://doi.org/10.4049/jimmunol.1500859.
43. Maarifi GSN, Maillet S, Moncorgé O, Chamontin C, Edouard J, Sohm F, Blanchet FP, Herbeuval JP, Lutfalla G, Levraud JP, Arhel NJ, Nisole S. 2019. TRIM8 is required for virus-induced IFN response in human plasmacytoid dendritic cells. Sci Adv 5:aax3511. https://doi.org/10.1126/sciadv.aax3511.
44. Ye W, Hu MM, Lei CQ, Zhou Q, Lin H, Sun MS, Shu HB. 2017. TRIM8 negatively regulates TLR3/4-mediated innate immune response by blocking TRIF-TBK1 interaction. J Immunol 199:1856–1864. https://doi.org/10.4049/jimmunol.1601647.
45. Qin Y, Zhou MT, Hu MM, Hu YH, Zhang J, Guo L, Zhong B, Shu HB. 2014. RNF26 temporally regulates virus-triggered type I interferon induction by two distinct mechanisms. PLoS Pathog 10:e1004358. https://doi.org/10.1371/journal.ppat.1004358.
46. Geahlen RL. 2014. Getting Syk: spleen tyrosine kinase as a therapeutic target. Trends Pharmacol Sci 35:414–422. https://doi.org/10.1016/j.tips.2014.05.007.
47. Hamerman JA, Tchao NK, Lowell CA, Lanier LL. 2005. Enhanced Toll-like receptor responses in the absence of signaling adaptor DAP12. Nat Immunol 6:579–586. https://doi.org/10.1038/ni1204.
48. Liu Y, Li R, Chen XX, Zhi Y, Deng R, Zhou EM, Qiao S, Zhang G. 2019. Non-muscle myosin heavy chain IIA recognizes sialic acids on sialylated RNA viruses to suppress proinflammatory responses via the DAP12-Syk pathway. mBio 10:e00574-19. https://doi.org/10.1128/mBio.00574-19.
49. Zhu Y, Wang R, Yu L, Sun H, Tian S, Li P, Jin M, Chen H, Ma W, Zhou H. 2020. Human TRA2A determines influenza A virus host adaptation by regulating viral mRNA splicing. Sci Adv 6:eaaz5764. https://doi.org/10.1126/sciadv.aaz5764.
50. Lee CM, Weight AK, Haldar J, Wang L, Klibanov AM, Chen J. 2012. Polymer-attached zanamivir inhibits synergistically both early and late stages of influenza virus infection. Proc Natl Acad Sci U S A 109:20385–20390. https://doi.org/10.1073/pnas.1219155109.
51. Xiao M, Chen Y, Wang S, Liu S, Rai KR, Chen B, Li F, Li Y, Maarouf M, Chen JL. 2021. LncRNA IFITM4P regulates host antiviral responses by acting as a ceRNA. J Virol 95:e00277-21. https://doi.org/10.1128/JVI.00277-21.
52. Li X, Guo G, Lu M, Chai W, Li Y, Tong X, Li J, Jia X, Liu W, Qi D, Ye X. 2019. Long noncoding RNA Lnc-MxA inhibits beta interferon transcription by forming RNA-DNA triplexes at its promoter. J Virol 93:e00786-19. https://doi.org/10.1128/JVI.00786-19.
53. Chen B, Chen Y, Rai KR, Wang X, Liu S, Li Y, Xiao M, Ma Y, Wang G, Guo G, Huang S, Chen J-L. 2021. Deficiency of eIF4B increases mouse mortality and impairs antiviral immunity. Front Immunol 12:54–57. https://doi.org/10.3389/fimmu.2021.723885.